

# Enhanced orbit determination for BeiDou satellites with FengYun-3C onboard GNSS data

Qile Zhao<sup>1,2</sup> · Chen Wang<sup>1</sup> · Jing Guo<sup>1</sup>  · Guanglin Yang<sup>3</sup> · Mi Liao<sup>3</sup> · Hongyang Ma<sup>1</sup> · Jingnan Liu<sup>1,2</sup>

Received: 3 September 2016 / Accepted: 27 January 2017 / Published online: 3 February 2017  
© The Author(s) 2017. This article is published with open access at Springerlink.com

**Abstract** A key limitation for precise orbit determination of BeiDou satellites, particularly for satellites in geostationary orbit (GEO), is the relative weak geometry of ground stations. Fortunately, data from a low earth orbiting satellite with an onboard GNSS receiver can improve the geometry of GNSS orbit determination compared to using only ground data. The Chinese FengYun-3C (FY3C) satellite carries the GNSS Occultation Sounder equipment with both dual-frequency GPS (L1 and L2) and BeiDou (B1 and B2) tracking capacity. The satellite-induced variations in pseudoranges have been estimated from multipath observables using an elevation-dependent piece-wise linear model, in which the constant biases, i.e., ambiguities and hardware delays, have been removed. For IGSO and MEO satellites, these variations can be seen in onboard B1 and B2 code measurements with elevation above 40°. For GEO satellites, a different behavior has been observed for these signals. The GEO B2 pseudoranges variations are similar to those of IGSO satellites, but no elevation-dependent variations have been identified for GEO B1. A possible cause is contamination of the larger noise in GEO B1 signals. Two sets of precise orbits were determined for FY3C in March 2015 using onboard GPS-only data and onboard BeiDou-only data, respectively. The 3D RMS

(Root Mean Square) of overlapping orbit differences (OODs) is 2.3 cm for GPS-only solution. The 3D RMS of orbit differences between BeiDou-only and GPS-only solutions is 15.8 cm. Also, precise orbits and clocks for BeiDou satellites were determined based on 97 global (termed GN) or 15 regional (termed RN) ground stations. Furthermore, also using FY3C onboard BeiDou data, two additional sets of BeiDou orbit and clock products are determined with the data from global (termed GW) or regional (termed RW) stations. In general, the OODs decrease for BeiDou satellites, particularly for GEO satellites, when the FY3C onboard BeiDou data are added. The 3D OODs reductions are 10.0 and 291.2 cm for GW and RW GEO solution with respect to GN and RN solution, respectively. Since the OODs in the along-track direction dominate the OODs reduction, no improvement has been observed by satellite laser ranging, which mainly validates the accuracy of the radial orbital component. With the GW BeiDou orbit and clock products, the FY3C orbits determined with onboard BeiDou-only data also show improvement in comparison with those determined with BeiDou GN products.

**Keywords** BeiDou · FengYun-3C · Precise orbit determination · Multipath combination · Code measurement

✉ Jing Guo  
jingguo@whu.edu.cn

<sup>1</sup> GNSS Research Center, Wuhan University, No. 129 Luoyu Road, Wuhan 430079, China  
<sup>2</sup> Collaborative Innovation Center of Geospatial Technology, Wuhan University, No. 129 Luoyu Road, Wuhan 430079, China  
<sup>3</sup> National Satellite Meteorological Center, No. 46, Zhongguancun South Street, Beijing 100044, China

## Introduction

Currently, the Chinese BeiDou Navigation Satellite System (BeiDou) consists of Geostationary Earth Orbit (GEO) satellites C01, C02, C03, C04 and C05, Inclined Geosynchronous Orbit (IGSO) satellites C06, C07, C08, C09 and C10, and Medium Earth Orbit (MEO) satellites C11, C12

and C14. BeiDou satellite orbits, as determined with observations from ground stations, suffer from problems in attitude control mode (Montenbruck et al. 2015), solar radiation pressure (SRP) modeling (Guo et al. 2016a), systematic errors in pseudoranges (Wanninger and Beer 2015), and geometry conditions (Zhao et al. 2013).

For BeiDou IGSO and MEO satellites, which use two attitude modes, namely yaw-steering (YS) and orbit-normal (ON) mode, dramatic orbit degradation can be observed when satellites switch the attitude mode or are in the ON mode. Based on studies with the yaw attitude model for BeiDou IGSO and MEO satellites (Feng et al. 2014; Guo et al. 2016b), efforts have been made to construct a better SRP model for these satellites in ON mode and at the attitude transit epoch (Guo 2014; Guo et al. 2016a; Prange et al. 2016). Although the orbit accuracy in ON mode can be improved, the orbit quality for the orbital arc containing the attitude transit epoch is still poor. Guo et al. (2016a) further identified the deficiency of the purely empirical CODE SRP model (Beutler et al. 1994; Springer et al. 1999) for BeiDou IGSO satellites in YS mode, and proposed the box-wing model as a priori SRP model to improve the CODE SRP model. In addition to this attitude and SRP issues, Wanninger and Beer (2015) identified satellite-induced variations in code measurements, termed code biases hereafter, which limit the ambiguity resolution when using the geometry-free approach. Furthermore, they also proposed an elevation-dependent model to correct the satellite-deduced code biases.

Compared with IGSO and MEO satellites, the BeiDou GEO orbits have relative poor quality as shown in Guo et al. (2016b). The main reason is that the GEO satellite ground tracks are relatively static, resulting in almost static observation geometry. Also, the ON model has been applied to GEO satellites (Montenbruck et al. 2015), but it makes the SRP acting on the satellites hard to model. Guo et al. (2016b) identified errors that noticeable depend on the orbital angle, i.e., the argument angle of the satellite with respect to the midnight point in the orbit plane, and large bias of about  $-40$  cm in satellite laser ranging (SLR) residuals. These errors are a result of using the empirical CODE SRP model. Liu et al. (2016) reported that GEO orbits could be improved by estimating six parameters instead of the typical five parameters of the empirical CODE SRP model. With this model, the bias of SLR residuals is only about  $-7.8$  cm for 28-day solutions. However, no significant improvement has been observed after incorporating the model into the Position And Navigation Data Analyst (PANDA) software (Liu and Ge 2003). Although elevation-dependent satellite-induced code biases were identified for IGSO and MEO satellites (Wanninger and Beer 2015), such biases cannot be seen for GEO satellites using ground tracking data only. The cause is

mainly the relative static geometry between GEO satellites and ground stations. Hence, it should be possible to improve the GEO orbits with onboard BeiDou tracking data from Low Earth Orbiters (LEOs), since the relative movement between GEO and LEOs results in the desired rapid change of observation geometry.

The idea of overcoming GNSS POD weakness due to small number of ground stations, poor distribution of ground stations, and poor geometry condition using LEOs onboard tracking data has been assessed previously (Geng et al. 2011; Zoulida et al. 2016). When onboard GPS data of GRACE A are combined with data from 43 ground stations, the 1D GPS orbit differences with respect to the IGS final orbit decreased to 5.5 from 8.0 cm (Geng et al. 2011). Also, when more LEOs are used, less ground stations are needed to achieve similar orbit accuracy as obtained without LEOs onboard data (Geng et al. 2011). The LEO onboard GPS data can also be used to estimate phase center corrections or to improve the reference frame (Haines et al. 2015). Previous research has focused on LEO onboard GPS data since there were no onboard data available for other GNSS systems. Thanks to the FengYun-3C (FY3C) satellite, onboard BeiDou data are collected and can be used for these investigations.

The aim of this study is to improve the BeiDou orbits by combining ground data and FY3C onboard tracking data, called here enhanced POD, and to analyze the elevation-dependent code biases of BeiDou satellites, particularly for GEO satellites. Following the introduction of the FY3C satellite and its onboard GNSS receiver, the quality of the collected data and the multipath errors will be investigated and analyzed. Afterward, the POD for FY3C with onboard GPS-only data or onboard BeiDou-only data will be presented, followed by a section on POD for BeiDou satellites combining ground BeiDou data and FY3C onboard BeiDou data. The thus determined BeiDou orbits and clocks will be validated by overlapping orbit comparison, by SLR, and by determination of FY3C orbits.

### FY3C satellite

The FY3C satellite was launched on September 23, 2013, and developed by the Meteorological Administration/National Satellite Meteorological Center (CMA/NSMC) of China. This satellite is in a sun-synchronous orbit with orbit altitude and inclination of about 836 km and  $98.75^\circ$ . The primary mission of FY3C is scientific investigation of atmospheric physics, weather, climate, electron density, magnetosphere, and troposphere as well as stratosphere exchanges (Bi et al. 2012). A GNSS Occultation Sounder (GNOS) has been placed on the satellite to ensure that the objectives can be achieved.

The GNOS instrument was developed by the Center for Space Science and Applied Research (CSSAR) of the Chinese Academy of Sciences (CAS). Three GNSS antennas, namely the PA (Positioning Antenna), the ROA (Rising Occultation Antenna), and the SOA (Setting Occultation Antenna) were installed on GNOS. The PA can track up to six BeiDou satellites and more than eight GPS satellites. The collected pseudoranges and carrier phases are used for real-time navigation, positioning, and POD of FY3C. The along-velocity viewing antenna ROA and anti-velocity viewing antennas SOA are used for rising and setting occultation tracking; however, only four BeiDou and six GPS occultations can be tracked simultaneously (Bai et al. 2014). In this study, we only used data from the PA for analysis.

Figure 1 shows a schematic view of the FY3C satellite. Table 1 lists the coordinates of the PA antenna reference point (ARP) in the satellite reference frame (SRF). The phase center offsets (PCOs) for GPS L1 and L2 signals in ARP are also presented. CMA/NSMC provided these values. Since no PCOs for BeiDou signals and phase center variations (PCVs) for GPS/BeiDou are provided, we assume that the BeiDou PCOs are same as those of GPS; the GPS/BeiDou PCVs are set as zero. As to satellite attitude, we simply assume that the satellite is flying with a fixed orientation coinciding with the SRF. The SRF is defined as follows: the origin is at the center of mass of the satellite, Z-axis points to the earth, the X-axis is perpendicular to the Z-axis and points to the direction of velocity, and the Y-axis completes the right-hand reference frame.

### Quality of FY3C onboard GPS and BeiDou data

In this section, we will assess the quality of FY3C onboard GPS and BeiDou data with emphasis on the elevation-dependent satellite-induced code biases, particularly for BeiDou GEO satellites.

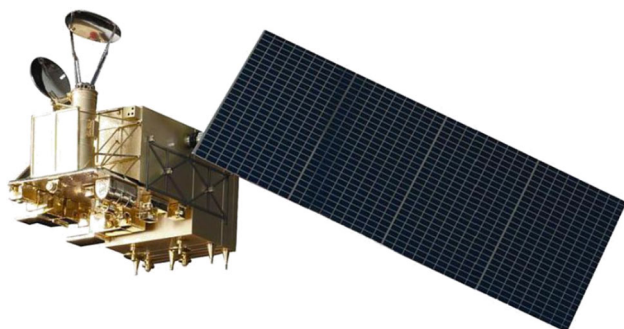


Fig. 1 FY3C satellite

**Table 1** Coordinates of the PA ARP in the SRF, and PCO for GPS L1 and L2 signals

	X (mm)	Y (mm)	Z (mm)
Coordinates of PA ARP in SRF	−1275.0	282.0	−983.7
PCOs of GPS L1	−5.0	0.0	15.0
PCOs of GPS L2	−3.0	0.0	15.0

### Data availability

We use 1 month of data during Day Of Year (DOY) 60–90, 2015, kindly provided by CSSAR. These data are recorded in the RINEX 2.1 files with 1 Hz and 30 s sampling rate for BeiDou and GPS, respectively. The following measurements for GPS and BeiDou satellites are available: (1) L1 C/A code, (2) L1 carrier phase, (3) L1 signal amplitude, (4) L2 P code, (5) L2 carrier phase, (7) L2 signal amplitude, (8) B1I code phase, (9) B1 carrier phase, (10) B1 signal amplitude, (11) B2I code phase, (12) B2 carrier phase, and (13) B2 signal amplitude. According to Bai et al. (2014), the precision of pseudorange and phase observables is less than 30 and 2 mm, respectively.

Figure 2 shows the number of measurements in DOY 60, 2015 for GPS and BeiDou. Compared to GPS CA/L1, more tracking losses in GPS P2/L2 observables can be observed. This can probability be attributed to the weak

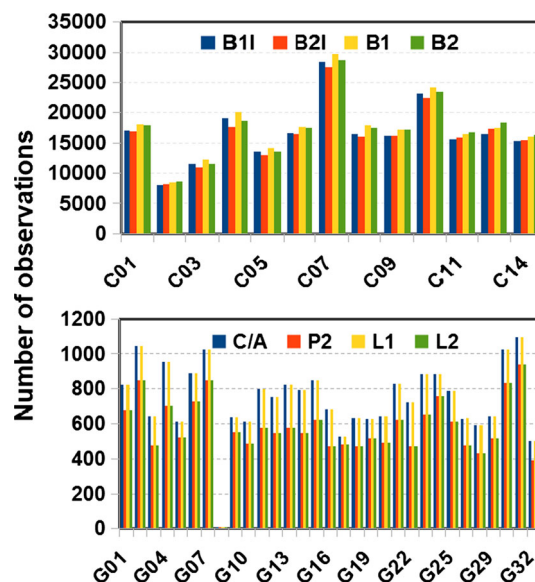


**Fig. 2** Observations collected by the FY3C onboard GNOS receiver for DOY 60, 2015. *Top* BeiDou B1I (blue) and BeiDou B2I (orange) code measurements, as well as BeiDou B1 (yellow) and BeiDou B2 (green) phase observations. *Bottom* GPS C/A (blue) and GPS P2 (orange) code measurements, as well as L1 (yellow) and L2 (green) carrier phase observations. No measurements for G26

acquisition of P2/L2 measurements in low elevation. In addition, the lower designed transmitting power for L2 makes the signals prone to loss. For BeiDou, there is more tracking loss in B1 than in B2 due to the relative greater transmitted power in B2. Also, we see that the number of BeiDou code measurement is less than that of the phase observables. For the GNSS receiver, since the satellite transmission signal structure is known, the code measurement is used to acquire the phase. Hence, generally, the number of phases should not be greater than that of pseudorange measurements. The lesser number of code measurements is caused by a bug in the decode software.

Figure 3 demonstrates the ratio of lost epochs to all epochs for each day as the indicator of data loss. In general, GPS observations are available 31 days. The loss percentage is less than 5%, except on DOY 063, 065, 074, 075, and 088. Among those days, the greatest loss percentage reaches up to 29.1% for DOY 074, which has a negative impact on orbit solution. By contrast, the BeiDou data loss percentage is about 20% for most of days, and reaches 87.5 and 65.0% for DOY 061 and 076. There is almost no data available in DOY 074. The relative greater data loss percentage for BeiDou indicates that this receiver has lower performance tracking the BeiDou signals. This will affect the quality of orbit determined with BeiDou-only data.

## Multipath

The multipath combinations (MPCs) are constructed based on algorithms used in TEQC (Estey and Meerten 1999) using single-frequency code measurements and dual-frequency phase measurements of a continuous ambiguity arc. The constant biases, such as ambiguities, hardware delay in satellite and receiver are removed by averaging the MPCs of an ambiguity arc. Using MPCs of BeiDou measurements from IGS MGEX stations, Wanninger and Beer (2015) identified that elevation-dependent biases influence the pseudoranges of BeiDou MEO and IGSO. Since the GEO satellites barely move relative to the static ground receiver,

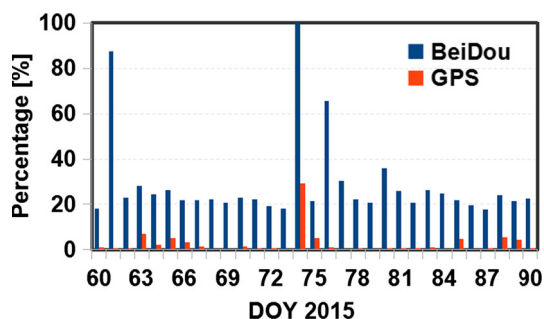


**Fig. 3** FY3C onboard BeiDou (blue) and GPS (orange) data loss percentage for each day during DOY 60–90, 2015

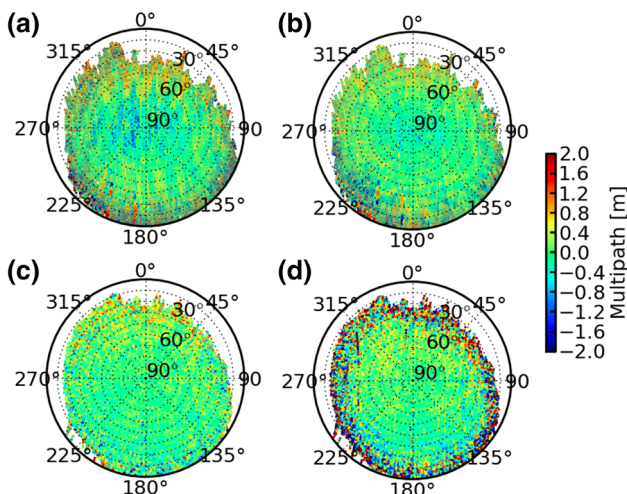
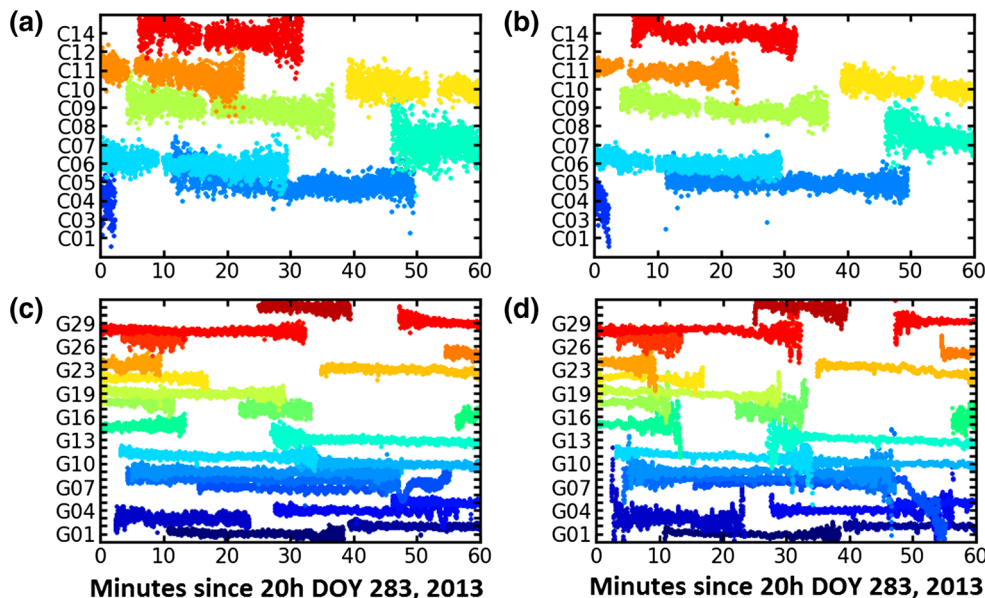
the biases in MPCs can absorb the biases in code measurements. Hence, the biases of BeiDou GEO code measurements cannot be identified with data from static ground receivers. The FY3C provides an essential way to overcome the dilemma.

Figure 4 shows the MPCs time series for FY3C onboard observations during the time 20–21 h of DOY 283, 2013, in which the 1 Hz onboard GPS and BeiDou observables are provided by CSSAR. In the figure, the interval between two consecutive PRN numbers along the vertical axis is 1 m. Panels (a) and (b) show the MPCs of BeiDou B1I and B2I, whereas the GPS C/A and P2 MPCs are plotted in panels (c) and (d). In general, the tracking duration for GPS and the different types of BeiDou satellites is about 30 min. For BeiDou, the MPCs of B1I are larger than those of B2I. For GPS, the MPCs of P2 are smaller than those of C/A in the high elevation, but much noisier in low elevation. The larger MPCs of BeiDou compared to those of GPS are also caused by the larger noise of BeiDou observables. A noticeable phenomenon is that the BeiDou observations are easily interrupted at high elevation. This problem is caused by the decode software developed and run by CSSAR. Contrary to BeiDou, the MPCs of GPS C/A and P2 are rather stable, and no gaps are observed in high elevation. However, GPS P2 MPCs show dramatic variations during the ascent and descent of GPS satellites. This is caused by the larger noise of P2 pseudoranges at low elevation and indicates that the onboard receiver has poor GPS L2 signal tracking ability in low elevation.

Figure 5 displays the MPCs variations for FY3C onboard BeiDou B1I (a), B2I (b), GPS C/A (c), and P2 (d) code measurements as a function of elevation and azimuth in the sky plot for 1 month (DOY 60–90, 2015). Overall, the large multipath errors are mainly found in low elevation areas, particularly for GPS P2. This is an indication of the poor GPS L2 signal tracking ability mentioned above. Also, it is easy to see that the MPCs show different patterns for BeiDou B1I and B2I code observations. The BeiDou B1I multipath errors depend primarily on elevation and vary only gradually with azimuth. However, the distribution of errors is not strictly symmetric in azimuth. Considering the different behavior of the B2I MPCs, the origin of errors cannot be readily contributed to the cross-track between osculation antennas and PA, and needs further investigation. In general, the averaged RMSs of MPCs for FY3C onboard BeiDou B1I, B2I, GPS C/A, and P2 code measurements are 0.69, 0.62, 0.38 and 0.820 m, respectively. Due to contamination by the larger noise of GPS P2 in the low elevation, the precision of pseudoranges is assessed with the MPCs above 40°. They are 0.50, 0.43, 0.28, and 0.37 m for BeiDou B1I, B2I, GPS C/A, and P2. The precision of GPS code measurement is



**Fig. 4** Time series of MPCs of BeiDou B1I (a), BeiDou B2I (b), GPS C/A (c), and GPS P2 (d) code measurements of FY3C onboard GNOS receiver. C02, G20 and G30 are not tracked in the selected period. The time is in minutes



**Fig. 5** Sky-plots of MPCs of BeiDou B1I (a), BeiDou B2I (b), GPS C/A (c), and GPS P2 (d) code measurements of FY3C onboard GNOS receiver

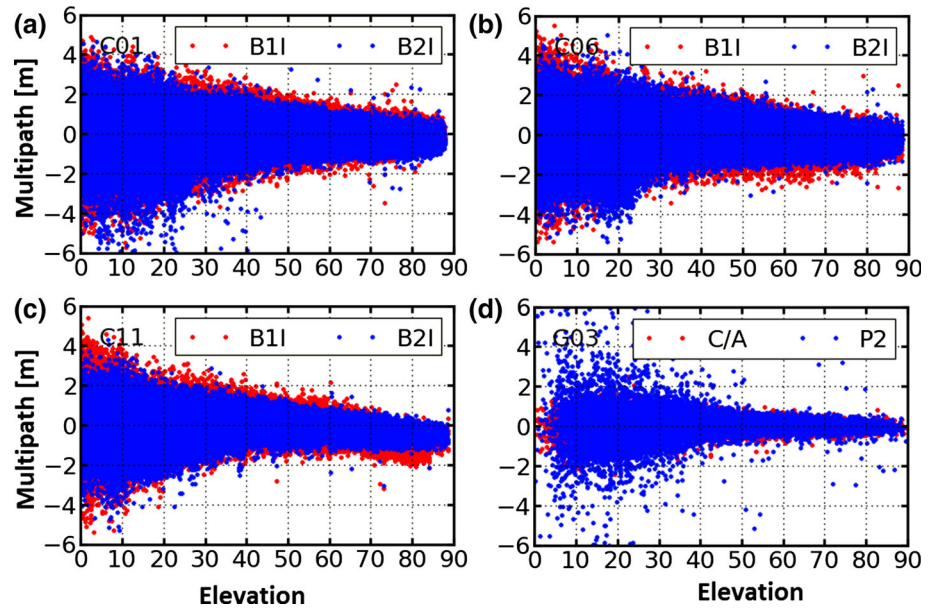
consistent with the reported 0.3 m value, but those for BeiDou are slightly worse.

Figure 6 shows the MPCs for BeiDou GEO C01 (a), IGSO C06 (b), MEO C11 (c), and GPS G03 (d) as a function of elevation. As demonstrated in Fig. 4, the noise level of BeiDou is greater than that of GPS. The BeiDou B2I and GPS C/A signals are better than BeiDou B1I and GPS P2, respectively. Compared with GEO and IGSO satellites, the MPCs of BeiDou MEO satellites show the clear elevation-dependent biases, particularly in higher elevations. To analyze these biases further, the elevation-dependent piece-wise linear models are estimated by using the approach of Wanninger and Beer (2015). We fitted the

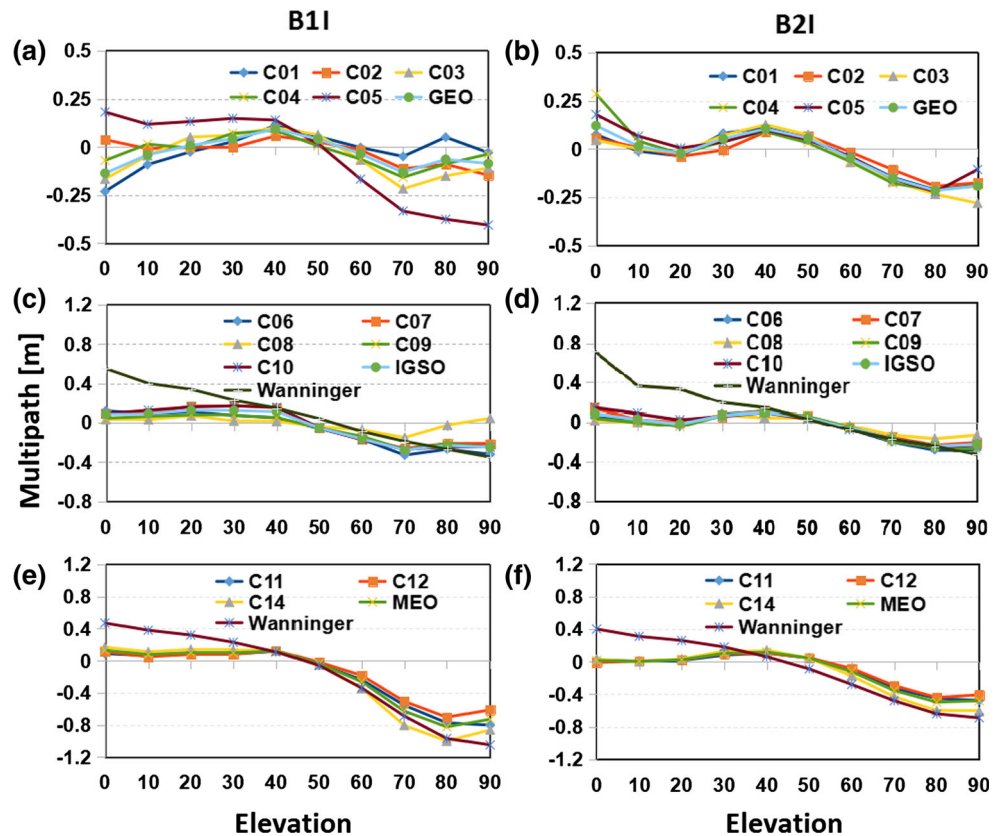
models for each BeiDou satellite and for the respective group classified according to the satellite types (i.e., GEO, IGSO, and MEO), with 1 month of MPCs data, and for each of the two BeiDou frequencies. Figure 7 shows the fitted elevation-dependent models. The upper (a and b), middle (c and d), and bottom (e and f) panels show the results for each satellite and the corresponding group, respectively. The left and right three panels demonstrate the results for B1I and B2I. For comparison, the IGSO and MEO group models from Wanninger and Beer (2015) are also illustrated. Since the B1I MPCs of C05 and C08 show significant departure compared to others, they have not been used to derive the corresponding piece-wise model for GEO and IGSO group.

Figure 7 shows similar variations for the fitted elevation-dependent models. Specifically, the bias is near zero at zero elevation, and gradually varies to reach maximum at about 40°, afterward decrease to the minimum with increasing elevation. However, the biases depend on satellite-type and frequency. The B1I biases are larger than those of B2I, particularly for MEO satellites. Compared with B1I, the B2I piece-wise models for individual BeiDou satellites show better consistency, particularly for MEO satellites thanks to the lower noise of B2I. It is interesting to note that the derived B2I MPCs model for the GEO and IGSO groups are almost the same, though the GEO and IGSO’s B1I models show different results. However, the variation of the C05 B1I model is similar as that of IGSO satellites. The different behavior for B1I and B2I can be contributed to the relative larger noise of B1I, which contaminates the elevation-dependent model estimation. Also, the differences between these fitted elevation-dependent models and Wanninger and Beer’s models for the

**Fig. 6** MPCs of BeiDou GEO C01 (a), IGSO C06 (b), MEO C11 (c), and GPS G03 satellite as a function of elevation. The red and blue dots represent B1I and B2I for BeiDou as well as C/A and P2 for GPS



**Fig. 7** Elevation-dependent MPC biases for BeiDou code observations. The upper (a, b), middle (c, d), and bottom (e, f) panels show the results for each GEO, IGSO, and MEO satellite and each group of BeiDou satellites, respectively. The left and right three panels demonstrate results for B1I and B2I



IGSO and MEO group are also clear, particularly for low elevation from zero to 40°. In the Wanninger and Beer model, clear linear variations are seen, whereas almost stable variations are derived from FY3C onboard BeiDou data in the low elevation. However, once the elevation is 40° and higher the two models are consistent, particularly

for IGSO B2 MPCs. This may be attributable to the fact that the FY3C GNOS receiver smoothed the BeiDou signals for elevation below 40°. Repeating this analysis for one week of data from DOY 283–289, 2013, shows similar results and the differences between corresponding model parameters are only marginal.

## Precise orbit determination for FY3C with onboard GPS and BeiDou data

Two sets of FY3C precise orbits have been determined with onboard GPS-only data and onboard BeiDou-only data from DOY 60–88, 2015. For the case of GPS-only data, the IGS final orbit and 30 s clock products were used. For the BeiDou-only solution, the BeiDou orbits and 30 s clocks determined with ground station data, i.e., the GN solution discussed in next section, were used.

Since no SLR measurements are available for FY3C, the determined orbits will be validated by orbit comparison in radial, along-track, cross-track, and 3D direction. For FY3C GPS-only solution, as the length of a POD arc is 30 h, i.e., from 21:00 of the first day to 3:00 of the third day, the 6-h overlapping orbit differences (OODs) of two consecutive orbit solutions are used for validation. In case of BeiDou-only solution, we directly compare the entire 30-h orbit positions of each the GPS-only and BeiDou-only POD arc.

### Strategy

We determine the dynamic orbits for FY3C, and carefully model the perturbation forces acting on the satellite to achieve the best solution. Table 2 summarizes the strategy used for POD in detail.

### Results and analysis

Figure 8 illustrates the daily RMS of orbit differences for the two solutions. For GPS-only solution (top), the 6-h OODs are quite small. Except in DOY 075 and 088, the daily RMS in each direction is below 30 mm, particularly it is about 1.0 cm in radial and cross-track component. The larger OODs are clearly dependent on the percentage of data loss, particularly for DOY 075, when about 29.1 and 5% data are lost in DOY 074 and 075. In general, the RMS of OODs reaches 1.9, 0.7, 0.8, and 2.3 cm in along-track, cross-track, radial, and 3D, respectively. The good orbit quality indicates an excellent performance of the FY3C onboard GNOS receiver.

Figure 8 (bottom) shows that the orbit differences for BeiDou-only solution are worse compared to GPS-only. The main reason is fewer BeiDou measurements, and lower accuracy of BeiDou orbit and clock products, particularly for GEO satellites. Also, the fewer data limit the dynamic parameters to be estimated in shorter duration. The mis-modeled dynamic force errors are reflected by the orbit differences in the along-track component. For most days, the 3D daily RMS varies between 10 and 30 cm. However, the orbit quality degrades significantly for DOY 061, 073,

075 and 076, as more than 60% data are lost in DOY 061, 074, and 076. A relative low performance is also seen for solutions in DOY 079 and 080 as 35% BeiDou data are lost in DOY 080. On average, the RMS of orbit differences with respect to the GPS-only solutions is about 13.6, 5.8, 4.9, and 15.8 cm in along-track, cross-track, radial, and 3D, respectively, once the arcs with greater data loss percentage (i.e., DOY 061, 073, 075, and 076) have been removed.

### Enhanced POD for BeiDou with FY3C onboard data

Two steps have been used for BeiDou POD. First, we use 3-day GPS data from the IGS MGEX network, the BeiDou Experimental Tracking Network (BETN), and FY3C onboard GPS data. Using IGS final GPS orbits, 30 s clocks and IERS Earth Rotation Parameters (ERP) products, we produce static PPP solutions for ground sites and FY3C dynamic orbits.

Second, the ground BeiDou data and FY3C onboard BeiDou data are used for BeiDou POD. The station positions and FY3C dynamic orbits, troposphere delay, and receiver clock obtained in the previous GPS-only PPP and FY3C GPS-only POD are introduced as known parameters. The estimated parameters for this solution include BeiDou satellite orbital parameters with respect to their initial broadcast ephemeris values, satellite clock offsets, float ambiguities and inter-system biases (ISB). We follow the recommendations of second IGS reprocessing campaign regarding the specific measurement model, reference frame, and orbit model. However, the earth radiation pressure and antenna thrust force are not included in orbit models for all solutions. The attitude model for the satellite bus follows the description in Guo et al. (2016a). Since the length of BeiDou tracking for the FY3C onboard receiver is less than 40 min, the data interval is set to 30 s for data processing to use more onboard BeiDou data.

We use global and regional data to analyze the contribution of FY3C onboard BeiDou data to BeiDou POD. Figure 9 illustrates the ground stations, where the blue and red cycles indicate the 97 global and 15 Asia–Pacific regional stations, respectively.

### Results and validation

Four sets of precise orbit and clock products for BeiDou satellites were determined from DOY 060 to 090, 2015 based on the global or regional ground stations with or without the FY3C onboard data. The corresponding acronyms are listed in Table 3. Since the length of BeiDou POD arc is 3 days, there are 48-h overlapping orbits for any two adjacent 3-day solutions shifted 1 day. Hence, in

**Table 2** Summary of POD strategy for FY3C

Geophysical models	Description
Static	Static part of EIGEN-6C up to degree and order 150
Temporal	Temporal part of EIGEN-6C up to degree and order 50
Secular rates for low degree coefficients	IERS Conventions 2010 (Petit and Luzum 2010)
N-body	JPL DE405
Solid earth tides	IERS Conventions 2010 (Petit and Luzum 2010)
Ocean tides	FES2004 (Lyard et al. 2006)
Ocean pole tides	Desai (2002)
Relativistic effects	IERS Conventions 2010 (Petit and Luzum 2010)
Satellite surface models and Attitude	
Atmospheric density	DTM94 (Berger et al. 1998)
Solar radiation pressure	Box-wing
Attitude	Nominal
Tracking data	
GPS/BeiDou	Undifferenced ionospheric-free phase and code (interval 30 s)
GPS orbits and clocks	IGS final orbits and 30 s final clock products
BeiDou orbits and clocks	Orbits and 30 s clocks determined with 97 ground station data (i.e., GN solution)
GPS antenna phase center correction	IGS08 (Schmid 2011)
BeiDou antenna phase center correction	Calibrated values (Guo et al. 2016b)
FY3C PCO and PCV	PCO listed in Table 1 for GPS and BeiDou; No PCV corrections
Weight	
GPS/BeiDou	2 cm for phase and 2 m for code measurements
Measurement parameters	
GPS/BeiDou	Real constant value for each ambiguity pass Epoch-wise receiver clock offset
Dynamical parameters	
GPS	Drag coefficient every 180 min One-cycle-per-orbit-revolution (1CPR) empirical accelerations in along- and cross-track every 180 min
BeiDou	Drag coefficient every 360 min 1CPR empirical accelerations in along- and cross-track every 900 min
POD arc length	30 h

this study, the 48-h OODs and SLR have been used to assess the BeiDou orbit quality. Furthermore, the POD for FY3C with its onboard BeiDou data is also used for validation of the determined BeiDou orbit and clock products.

Figure 10 illustrates the averaged 3D RMS of 48-h OODs for the four solutions. For the RN solution, the 3D RMSs of GEO satellites are above 100 cm, particularly for C02 and C05 the RMSs reach up to 700 cm. By contrast, for IGSO and MEO satellites, the averaged 3D RMSs are about 20–30 cm and about 20 cm, respectively. Once the FY3C onboard BeiDou data has been used for BeiDou POD, the 3D RMSs of OODs reduce due to improving the observation geometry. Compared to the RN solution, the averaged 3D RMS of RW solution reduces from 354.3 to

63.1 cm for GEO, 22.7 to 20.0 cm for IGSO, and 20.9 to 16.7 cm for MEO satellites. As expected, the greatest improvement has been achieved for GEO satellites, particularly for C02 and C05, since the inclusion of FY3C onboard BeiDou data strengthens the observation geometry. The improvement of IGSO orbit consistency is less than that of MEO, because the inclusion of FY3C onboard BeiDou data improves the MEO tracking capacity outside the Asia–Pacific region. For the two solutions with global stations, their OODs are smaller than those for the cases of regional stations. For GN solution, the averaged 3D RMSs of OODs are 53.3, 10.4, and 4.9 cm for GEO, IGSO, and MEO satellites; they show significant improvement with respect to the RN solution as expected. This indicates the



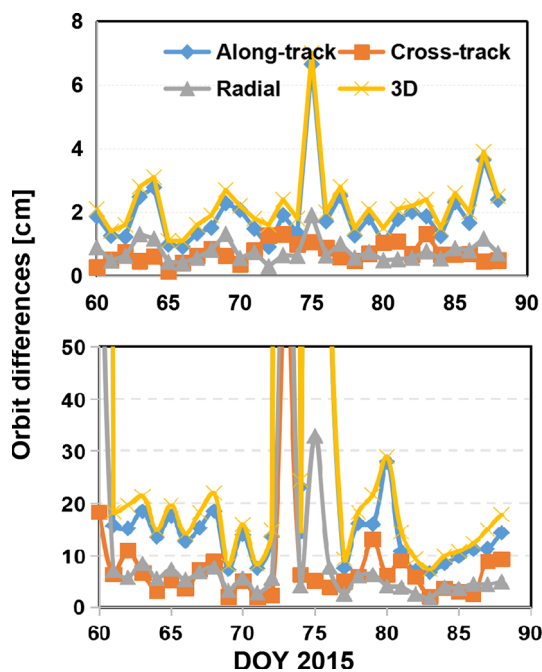


**Fig. 8** Daily RMS of orbit differences for FY3C GPS-only solution (top) and BeiDou-only solution (bottom)

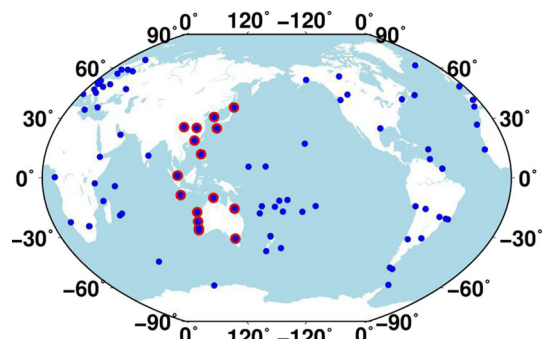


**Fig. 9** Distribution of ground sites used for BeiDou POD. The blue and red cycles indicate the 97 global and 15 regional stations, respectively

**Table 3** Acronyms for POD solutions of BeiDou satellites

Solution	Ground stations	FY3C onboard BeiDou data
GW	Global	With
GN	Global	Without
RW	Regional	With
RN	Regional	Without

inclusion of more ground stations can improve the BeiDou orbital quality. Once the FY3C onboard BeiDou observations are used, the 3D RMS of OODs can be further reduced to 43.4 cm for GEO satellites. However, almost the same RMSs of OODs have been found for the IGSO

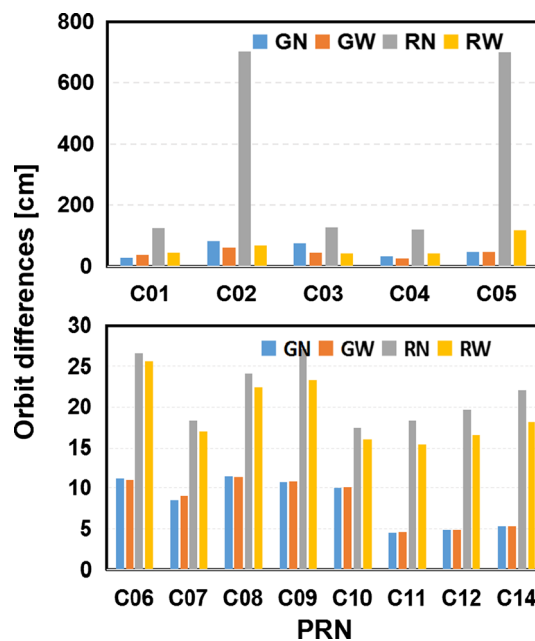


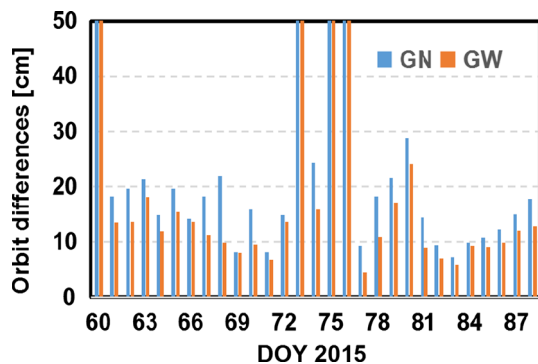
**Fig. 10** Averaged 3D RMS for 48-h OODs of four sets of FY3C BeiDou orbits. GEO (top), IGSO and MEO (bottom). The blue, red, gray, and orange one indicates the GN, GW, RN, and RW solution as listed in Table 3

and MEO orbits. In contrast to the RN and RW solutions, the BeiDou data from 97 global ground stations have been used for GN and GW solutions. These ground data play an important role in the GW solution and decrease the contribution of FY3C onboard BeiDou data for BeiDou POD, particularly for IGSO and MEO with good global tracking. Hence, almost no improvement has been observed for two global IGSO and MEO solutions, and the improved percentage of global GEO orbit solutions is less than that of regional solutions. Also, only six channels have been assigned for BeiDou tracking, resulting in less data available for BeiDou POD, and the tracking is easy to be interrupted when BeiDou satellites are in high elevation, as illustrated in Fig. 4. These two issues further weaken the contribution of FY3C onboard BeiDou data for BeiDou POD.

Since the length of a POD arc is 3 days, only the orbits in the middle day are used for SLR validation of C01, C08, C10, and C11 which are tracked by the International Laser Ranging Service (Pearlman et al. 2002). The SLR residuals exceeding an absolute value of 100 cm for GEO and 40 cm for IGSO and MEO are excluded in the validation. The corresponding results for GN and GW solution are listed in Table 4. Although inclusion of FY3C onboard BeiDou data has reduced the OODs of BeiDou orbits, the SLR validation indicates that almost the same accuracy has been achieved for all three kinds of BeiDou satellites, no matter whether or not the FY3C onboard BeiDou data are used. The same phenomena have also been found for RN and

**Table 4** Statistical results of SLR residuals for GN and GW solution (units: cm)

	C01		C08		C10		C11	
	GN	GW	GN	GW	GN	GW	GN	GW
Bias	-43.1	-43.1	-8.6	-8.6	-1.8	-1.7	-1.7	-1.7
STDev	12.3	13.1	3.4	3.4	4.6	4.7	8.9	8.9
RMS	44.8	45.0	9.2	9.2	4.8	4.9	9.0	9.0

**Fig. 11** Daily 3D RMS of orbit differences for the two sets of FY3C BeiDou-only orbits with respect to the GPS-only solution. The blue indicates the result for FY3C BeiDou-only orbit determined with GN solution, whereas the orange represents those determined with GW solution

RW solutions. The reason is that the OODs reduction in the along-track direction plays a dominating role, and almost no improvement is in the cross-track and radial components. However, the SLR is mainly used to validate the accuracy of radial orbit.

We determined the FY3C BeiDou-only dynamic orbits with GN and GW solutions to further assess the quality of BeiDou orbit and clock products. The daily 3D RMS of orbit differences for the two sets of FY3C BeiDou-only orbits with respect to the GPS-only solution is shown in Fig. 11. The improvement can be clearly observed for FY3C BeiDou-only orbits determined with GW solution. On average, the orbit differences have been reduced from 13.6 to 10.6 cm in along-track, 5.8 to 3.1 cm in cross-track, 4.9 to 3.8 cm in radial, and 15.8 to 11.7 cm in 3D, when the arcs with greater data loss percentage (i.e., DOY 061, 073, 075, and 076) have been removed. Hence, we find that the FY3C BeiDou onboard data contribute to improving the quality of BeiDou orbit and clock products.

## Conclusion

We use the FY3C onboard code and phase data to investigate the possibility of improving the geometric condition and BeiDou orbit as well as clock products. First, the

satellite-induced code biases have been investigated based on MPCs. It was confirmed that code biases are only seen in the onboard code measurements of BeiDou IGSO and MEO satellites with elevation above 40°. The consistency with the Wanninger and Beer (2015) model is quite good for those high-elevation observations. For GEO satellites, a different behavior has been seen for B1 and B2 signals. The variations of GEO B2 elevation-dependent errors in code are similar as that of IGSO B2 signals, whereas no elevation-dependent errors have been identified for GEO B1 signals. This is possibly caused by the contamination of greater noise in GEO B1 signals.

Using the onboard GPS and BeiDou data, the FY3C precise orbits have been determined with GPS-only data and BeiDou-only data. However, the orbital quality is easily affected by the available tracking data. The 3D RMS of 6-h OODs reaches 2.3 cm for GPS-only solution. The 3D RMS of orbit differences between BeiDou-only and GPS-only solutions is about 15.8 cm with removing the bad POD arcs.

Also, the precise orbits for BeiDou satellites have been determined with ground data from global or regional stations, in combination with or without FY3C onboard data. The 48-h OODs demonstrate that the orbit consistency improves for BeiDou satellites, particularly for GEO satellites, once FY3C onboard data are added. The improvements are mainly in the along-track direction. When fewer ground stations are used, a greater improvement can be achieved. With the enhanced BeiDou orbit and clock products, which are determined with global ground and FY3C onboard BeiDou data, the determined FY3C orbits with onboard BeiDou-only data show remarkable improvement. This provides a promising and a possible way for improving the BeiDou orbits and clocks with more LEO onboard data in the future, particularly in those situations where there is a small number of limited ground stations.

**Acknowledgements** The IGS MGEX, iGMAS, and ILRS are greatly acknowledged for providing the Multi-GNSS and SLR tracking data. The research is partially supported by the National Natural Science Foundation of China (Grant Nos. 41504009, 41574030). Finally, the authors are also grateful for the comments and remarks of reviewers and editor-in-chief, who helped to improve the manuscript significantly.

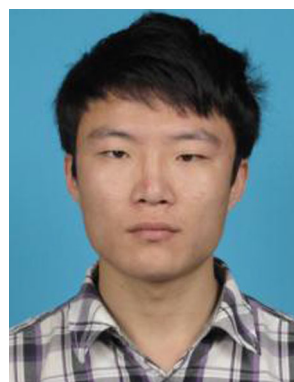
**Open Access** This article is distributed under the terms of the Creative Commons Attribution 4.0 International License (<http://creativecommons.org/licenses/by/4.0/>), which permits unrestricted use, distribution, and reproduction in any medium, provided you give appropriate credit to the original author(s) and the source, provide a link to the Creative Commons license, and indicate if changes were made.

## References

- Bai W, Sun Y, Du Q, Yang G, Yang Z, Zhang P, Bi Y, Wang X, Cheng C, Han Y (2014) An introduction to FY3 GNOS instrument and mountain-top test. *Atmos Meas Tech* 7:1817–1823. doi:10.5194/amt-7-1817-2014
- Berger C, Biancale R, Barlier M III (1998) Improvement of the empirical thermospheric model DTM: DTM94—a comparative review of various temporal variations and prospects in space geodesy applications. *J Geod* 72(3):161–178. doi:10.1007/s001900050158
- Beutler G, Brockmann E, Gurtner W, Hugentobler U, Mervart L, Rothacher M, Verdun A (1994) Extended orbit modeling techniques at the CODE processing center of the international GPS service for geodynamics (IGS): theory and initial results. *Manuscr Geod* 19(6):367–386
- Bi Y, Yang Z, Zhang P, Sun Y, Bai W, Du Q, Yang G, Chen J, Liao M (2012) An introduction to China FY3 radio occultation mission and its measurement simulation. *Adv Space Res* 49:1191–1197. doi:10.1016/j.asr.2012.01.014
- Desai S (2002) Observing the pole tide with satellite altimetry. *J Geophys Res* 107(C11):3186. doi:10.1029/2001JC001224
- Estey L, Meerten C (1999) TEQC: the multi-purpose toolkit for GPS/GLONASS data. *GPS Solut* 3(1):42–49. doi:10.1007/PL00012778
- Feng W, Guo X, Qiu H, Zhang J, Dong K (2014) A study of analytical solar radiation pressure modeling for BeiDou navigation satellites based on raytracking method. In: Sun J, Jiao W, Wu H, Shi C (eds) *Proceedings of the China Satellite Navigation Conference (CSNC) 2014*, vol. II. Lecture notes in electrical engineering 304:41–53. doi:10.1007/978-3-642-54743-0\_35
- Geng J, Shi C, Zhao Q, Ge M, Liu J (2011) Integrated adjustment of LEO and GPS in precise orbit determination. In: Xu P, Liu J, Dermanis A (eds) *VI Hotine-Marussi symposium on theoretical and computational geodesy*, volume 132 of the series international association of geodesy symposia, pp 133–137. doi:10.1007/978-3-540-74584-6\_20
- Guo J (2014) The impacts of attitude, solar radiation and function model on precise orbit determination for GNSS satellites. Ph.D. dissertation (in Chinese with English abstract), GNSS Research Center, Wuhan University, Wuhan, China
- Guo J, Chen G, Zhao Q, Liu J, Liu X (2016a) Comparison of solar radiation pressure models for BDS IGSO and MEO satellites with emphasis on improving orbit quality. *GPS Solut*. doi:10.1007/s10291-016-0540-2
- Guo J, Xu X, Zhao Q, Liu J (2016b) Precise orbit determination for quad-constellation satellites at Wuhan University: strategy, result validation, and comparison. *J Geod* 90(2):143–159. doi:10.1007/s00190-015-0862-9
- Haines B, Bar-Sever Y, Bertiger W, Desai S, Harvey N, Sibos A, Weiss J (2015) Realizing a terrestrial reference frame using the global positioning system. *J Geophys Res* 120(8):5911–5939. doi:10.1002/2015JB012225
- Liu J, Ge M (2003) PANDA software and its preliminary result of positioning and orbit determination. *Wuhan Univ J Nat Sci* 8:603–609. doi:10.1007/BF02899825
- Liu J, Gu D, Ju B, Shen Z, Lai Y, Yi D (2016) A new empirical solar radiation pressure model for BeiDou GEO satellites. *Adv Space Res* 57:234–244. doi:10.1016/j.asr.2015.10.043
- Lyard F, Lefevre F, Letellier T, Francis O (2006) Modelling the global ocean tides: modern insights from FES2004. *Ocean Dyn* 56(5):394–415. doi:10.1007/s10236-006-0086-x
- Montenbruck O, Kroes R (2003) In-flight performance analysis of the CHAMP BlackJack GPS receiver. *GPS Solut* 7(2):74–86. doi:10.1007/s10291-003-0055-5
- Montenbruck O, Schmid R, Mercier F, Steigenberger P, Noll C, Fatkulin R, Kogure S, Ganeshan AS (2015) GNSS satellite geometry and attitude models. *Adv Space Res* 56:1015–1029. doi:10.1016/j.asr.2015.06.019
- Pearlman M, Degnan J, Bosworth J (2002) The international laser ranging service. *Adv Space Res* 30:135–143. doi:10.1016/S0273-1177(02)00277-6
- Petit G, Luzum B, (2010) IERS conventions 2010, technical report. IERS Convention Center
- Prange L, Orliac E, Dach R, Arnold D, Beutler G, Schaer S, Jäggi A (2016) CODE’s five-system orbit and clock solution—the challenges of multi-GNSS data analysis. *J Geod*. doi:10.1007/s00190-016-0968-8
- Schmid R (2011) Upcoming switch to IGS08/igs08.atx—details on igs08.atx. IGSMAIL-6355. <http://igs.org/pipermail/igsmail/2011/006347.html>
- Springer T, Beutler G, Rothacher M (1999) A new solar radiation pressure model for GPS satellites. *GPS Solut* 2(3):50–62. doi:10.1007/PL00012757
- Wanninger L, Beer S (2015) BeiDou satellite-induced code pseudo-range variations: diagnosis and therapy. *GPS Solut* 19:639–648. doi:10.1007/s10291-014-0423-3
- Zhao Q, Guo J, Li M, Qu L, Hu Z, Shi C, Liu J (2013) Initial results of precise orbit and clock determination for COMPASS navigation satellite system. *J Geod* 87(5):475–486. doi:10.1007/s00190-013-0622-7
- Zoulida M, Pollet A, Coulot D, Perosanz F, Loyer S, Biancale R, Rebischung P (2016) Multi-technique combination of space geodesy observations: impact of the Jason-2 satellite on the GPS satellite orbits estimation. *Adv Space Res* 58:1376–1389. doi:10.1016/j.asr.2016.06.019



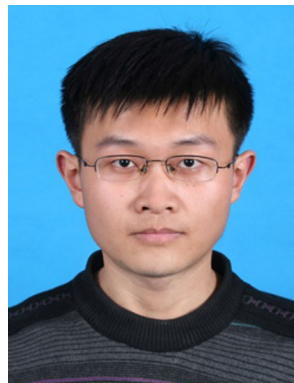
**Qile Zhao** is a professor at GNSS Research Center of Wuhan University. He received his Ph.D. degree at Wuhan University in 2004. In 2006–2007, as a postdoctoral fellow, he did his postdoctoral program in DEOS, Delft University of Technology, the Netherlands. His current research interests are precise orbit determination of GNSS and low earth orbiting satellites, and high-precision positioning using GPS, Galileo and BDS systems.



**Chen Wang** is a Ph.D. student at GNSS Research Center, Wuhan University currently. He received his bachelor degree at College of Geology Engineering and Geomatics, Chang’an University in 2014. His research focuses on GNSS data processing and orbit determination.



**Jing Guo** is a postdoctoral researcher at GNSS Research Center of Wuhan University. He received his bachelor, master and doctor degrees at Wuhan University in 2009, 2011 and 2014, respectively. Currently, he works on GNSS data processing, particularly the precise orbit determination for multi-GNSS satellites, and is also responsible for the routine data processing of MGEX and iGMAS at Wuhan University.



**Hongyang Ma** is a Ph.D. student at GNSS Research Center of Wuhan University. He obtained his M.S. degree with distinction in Geodesy and Engineering Surveying at the Institute of Geodesy and Geodynamics of Chinese Academy of Surveying and Mapping. His main research interests include precise orbit determination of GNSS satellites and precise point positioning.



**Guanglin Yang** received the M.S. degree in atmosphere physics from Peking University, Beijing, 2002. He is currently a senior engineer in ionospheric observation, working in national space weather center (China Meteorological Administration). His research interests include GNSS radio occultation, GNSS/MET and coupling of upper atmosphere and ionosphere.



**Jingnan Liu** graduated from the former Wuhan College of Surveying and Mapping in 1967 and received his master's degree in 1982. He was elected Academician of the Chinese Academy of Engineering in 1999. Since 1998, he has been in charge of the National Engineering Research Center for Satellite Positioning System. He has been a member of the Science and Technology Committee, Ministry of Education of China in 1997–2009 and as an editorial board member of GPS Solutions in 1998–2000. He is currently an executive member of the council, Chinese Society for Geodesy, Photogrammetry and Cartography; the editorial board member of GPS World; and the coordinator of IGS.



**Mi Liao** received the M.S. degree in atmospheric physics from Chinese Academy of Meteorological Science, Beijing, China, in 2011. Since then, she has been one of the members of radio occultation team in National Satellite Meteorological Center, China Meteorological Administration, Beijing. Her research interests include error analysis and application of RO data.